# Impact of Nonuniform Illumination and Probe Bar Shading on Solar Cell *I–V* Measurement

Samuel Raj, Jian Wei Ho, Johnson Wong, and Armin G. Aberle

***Abstract*—This paper examines the effect of nonuniform and probe-bar-shaded solar illumination in the *I–V* characterization of large area Si wafer solar cells. The illumination conditions were experimentally implemented by masking the solar cell during measurement. The results are examined in detail with simulations in Griddler, a finite element analysis software developed at the Solar Energy Research Institute of Singapore. The light *I–V* characteristics, particularly the fill factor, depend on the specific irradiance profiles relative to the current-collecting busbars due to effects on the effective series resistance $R_s$. The effect is slight for small light nonuniformities (IEC 60904 Class A nonuniformity classification or $<2\%$) but for light nonuniformities up to 20%, the standard deviation in the fill factor can reach about 0.19% absolute. Probe bar shading directly leads to an underestimation of the measured fill factor due to longer current paths and larger voltage drops.**

***Index Terms*—Current–voltage (*I–V*), Griddler, nonuniform illumination, probe bar shading, solar cell.**

## I. Introduction

The definition of standard testing conditions for solar cell current–voltage (*I–V*) measurements, precise definitions of the solar spectrum and classification of solar simulators [1], are consistent with the general motivation to render solar cell *I–V* testing a highly standardized and reproducible measurement between test laboratories. Most efforts in raising measurement accuracy, establishing traceability, and standardization focus on the prediction of device short-circuit current ($I_{sc}$) under the target spectrum [2]. Meanwhile, the cell open-circuit voltage ($V_{oc}$) is usually not sensitive to the probing configuration, and is accurate to within 0.5% uncertainty so long as the device temperature can be maintained to $\pm 1$°C. On the other hand, there is considerably less promotion of best practices toward obtaining *I–V* curves that yield accurate maximum power points (MPP) or fill factors (FF), although there are numerous factors related to light distribution and probing configuration that can impact these measured values. Implicitly, the ideal test condition of a solar cell prescribes close proximity of source and sense probes, identical voltages at current extraction points of like polarity, and perfectly uniform distribution of light over the cell plane. The impacts of deviations from these conditions have only been cursorily reported [3], while detailed work on the effects of nonuniform light illumination have mainly focused on concentrator solar cells [4], [5]. The goal of this work is to investigate the typically encountered spatial variations in illumination in the testing of large area Si wafer solar cells, and examine whether routine setups for *I–V* testing suffice in achieving accurate FF measurements.

There are namely two often encountered sources of light nonuniformity in the test cell plane: the first being nonuniformity in the incident light field itself, and the second being shading by the probe bars. Solar simulators that employ xenon short arc lamp, parabolic mirror, fly's eye integrator, and collimating lens can typically meet the 2% spatial uniformity requirements for class A categorization, although bulb misalignments, degradation in reflecting mirrors, nonuniformity developed in filtering elements, etc., can erode the spatial uniformity over time. Systems that employ more than one lamp, or an array of light emitting diodes (LEDs) which involve multiple illumination sources that need to be integrated and homogenized over the test plane, present further challenges to achieving the required light uniformity. Shading by probe bars is usually the result of finite probe bar thickness, misalignment between the probe bars and the cell busbars, bent probe bars made of printed circuit board or other flexible materials, and the casting of shadow due to large incident beam divergence. In the last scenario, if the beam divergence is 6°, a 5 cm high probe bar contacting the outer busbars of a three bus bar silicon wafer solar cell with 156 mm length would cast a shadow 1.45 mm wide. Probe bar shading can be avoided during the determination of $I_{sc}$, by making use of Kelvin probes which only contact the busbars near the wafer edges for current extraction, but the same current extraction near wafer edges cannot be used for the determination of the *I–V* curve MPP, as the cell busbars are typically not designed to conduct large currents.

This paper presents both experimental data on the variation of *I–V* parameters under different light distributions that might be encountered in realistic *I–V* testing conditions, as well as supplementary simulations using a detailed finite-element model [6], [7] of the solar cell plane under a large number of different possible light distributions. The latter simulations are useful toward establishing the statistical distribution in the *I–V*

Manuscript received March 20, 2017; accepted May 29, 2017. Date of publication July 24, 2017; date of current version August 18, 2017. This work was supported by the Solar Energy Research Institute of Singapore (SERIS). SERIS is supported in part by the National University of Singapore and in part by the Singapore's National Research Foundation through the Singapore Economic Development Board. *(Corresponding author: Samuel Raj.)*

S. Raj, J. W. Ho, and J. Wong are with the Solar Energy Research Institute of Singapore, National University of Singapore, 119077, Singapore (e-mail: samuelraj@nus.edu.sg; jw.ho@nus.edu.sg; johnson.wong@nus.edu.sg).

A. G. Aberle is with the Solar Energy Research Institute of Singapore and the Department of Electrical and Computer Engineering, National University of Singapore, 119077, Singapore (e-mail: armin.aberle@nus.edu.sg).

Color versions of one or more of the figures in this paper are available online at http://ieeexplore.ieee.org.

Digital Object Identifier 10.1109/JPHOTOV.2017.2726558

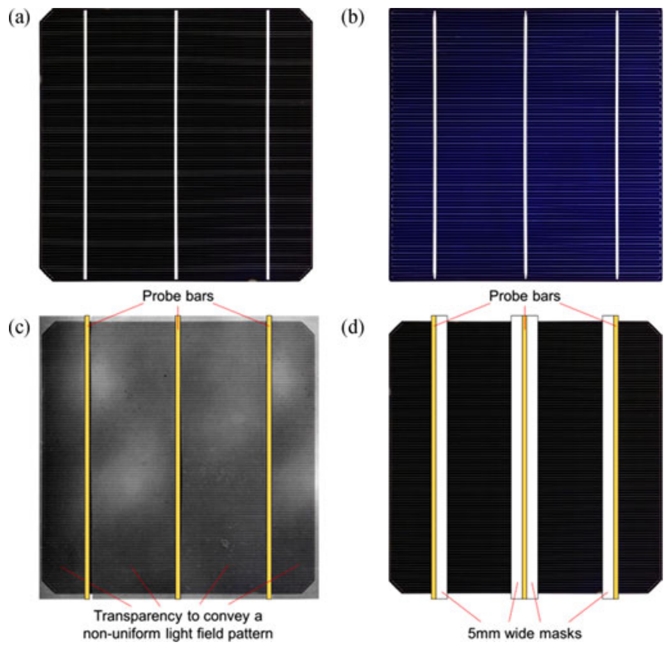


Fig. 1. (a) Monocrystalline and (b) multicrystalline Si wafer solar cells used as test cells in this work. (c) Nonuniform light field on a Si wafer solar cell created by overlaying a transparency with dot matrix pattern. (d) Large probe bar shading is affected by placing 5 mm wide masks on the sides of the probe bars.

parameters as a function of the degree of light nonuniformity, as it is possible to simulate a much larger number of scenarios than experiments would allow.

## II. Experimental Details

Two 156 × 156 mm Si wafer solar cells, one monocrystalline and one multicrystalline, as shown in Fig. 1(a) and (b), were used as test cells in this work. Both cells are p-type aluminum back surface field cells with fully metallized rear sides, and standard three-bus bar H-pattern metal grids on the front side. The front emitter sheet resistance is about 80 Ω/sq for both cells. The monocrystalline cell has been light soaked under 1 sun and 25°C for 48 h to ensure stability of effective recombination lifetime under further illumination during the experiment. *I–V* characteristics were measured by a long pulse LED solar simulator from WAVELABS (model: Sinus-220). The light engine consists of a honeycomb combination of 21 different colors of LEDs (wavelength ranging from 350 to 1050 nm) coupled with optics for uniform light irradiance ($<2\%$ nonuniformity) and is of class AAA according to IEC 60904-9 Ed. 2.0 [1].

Both cells have gone through *I–V* testing under best practice conditions, using a 156 × 156 mm pseudosquare monocrystalline Si wafer solar cell as the reference cell, with $I_{\rm sc}$ determined using a spectral mismatch factor corrected to AM1.5G according to IEC 60904-3 Ed. 2.0 [8], [9]. Both cells have had *I–V* testing done under the 2% uniform illumination as well as nonuniform light fields in the test plane.

Under repeatability tests, the *I–V* tester has lower than 0.05% standard deviation in the short-circuit current $I_{\rm sc}$, 0.5 mV standard deviation in open-circuit voltage $V_{\rm oc}$, and 0.005% standard deviation in FF if the probe bars were not moved between measurements. Therefore, one can expect to resolve *I–V* parameter variations as a result of different light distributions to the levels of these standard deviations.

Nonuniform incident light on the cell is created by placing a transparency with a printed dot matrix pattern with variable density, as shown in Fig. 1(c), on top of the cell. As a result of spectrally dependent transmittance of light through the transparency paper, one does not expect that the incident light on the cell to have class A spectral match to the AM1.5G spectrum in this case.

Probe bar shading is achieved by placing 5 mm wide opaque masks on the sides of the probe bars as shown in Fig. 1(d). In all cases, comparison of the *I–V* parameters is made by adjusting the illumination until the target $I_{\rm sc}$ is reached, thus ensuring that the total incident illumination power was similar and that only the spatial distribution was varied.

## III. Simulation Model

The monocrystalline cell has been characterized by taking photoluminescence (PL) images at different light intensities, while simultaneously probing the bus bar voltage. Its recombination parameters are estimated by simulating the PL images and voltages under these different light intensity illumination conditions using a dedicated finite-element simulator called Griddler 2 [6], [10]. The methods involved are detailed in [7]. Griddler 2 is also then used to simulate the *I–V* parameters of the monocrystalline cell under the various kinds of nonuniform light considered in this work. Griddler 2 represents the solar cell front plane as a large network of interconnected diodes, in a triangular mesh of about 80 000 nodes. Each node consists of a current source, which represents the light-induced current, whose value is equal to the node area times the local light-induced current density $J_L$. Griddler 2 has the capability to define the spatial distribution in $J_L$ across the cell plane at the resolution of the triangular elements, each of which is about 3 mm$^2$ large. The expected light distributions after placing the nonuniform transparency shown in Fig. 1(c), and after placing the 5 mm wide masks in Fig. 1(d), can be easily input to Griddler 2 to simulate the cell operating characteristics under such light distributions.

## IV. Results and Discussion

### A. Impact of Irradiance Nonuniformity on the Fill Factor of Solar Cells

The nonuniformity of the irradiance is defined in IEC 60904-9 [1] as

$$\text{Nonuniformity}\,(\%) = \frac{\text{max irradiance} - \text{min irradiance}}{\text{max irradiance} + \text{min irradiance}} \times 100\%. \quad (1)$$

Fig. 2 shows the FF for both monocrystalline and multicrystalline Si solar cells as a function of the short-circuit current ($I_{\rm sc}$) under the nonuniform light field (6% and 15% nonuniformity) and the deliberate shading at the probe bars mentioned in Fig. 1(c) and (d). The points on the graphs represent

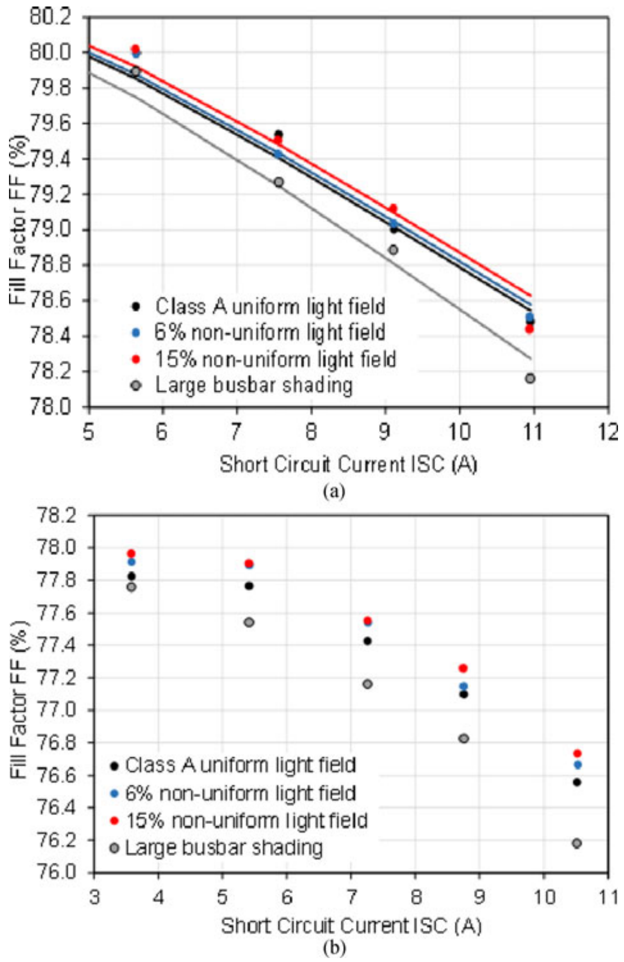


Fig. 2. Effect of nonuniform light fields and probe bar shading on the fill factor of the (a) monocrystalline and (b) multicrystalline Si solar cell.

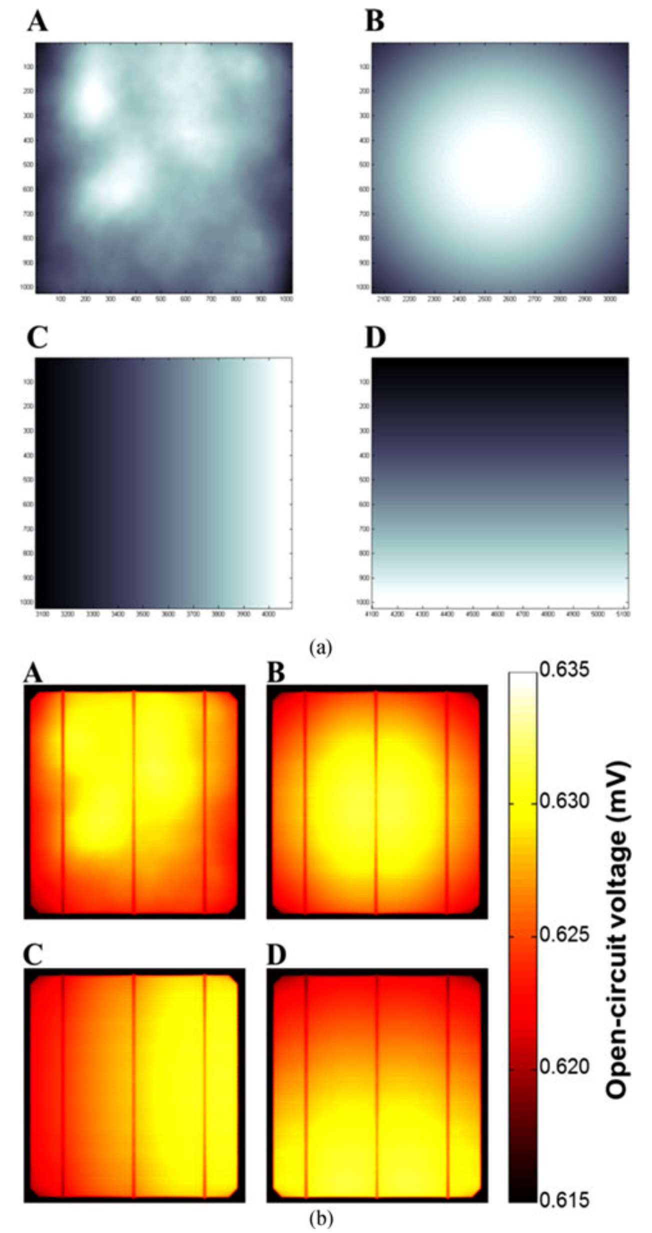


Fig. 3. (a) Four nonuniform irradiance profiles chosen for Griddler simulation. A: Light field as acquired from a PL imaging tool; B: Radial flat field; C: Horizontal linearly varying flat field; D: Vertical linearly varying flat field. (b) Simulated open-circuit voltage map arising from the nonuniform irradiance profiles in Fig. 4(a).

experimental data while the lines in Fig. 2(a) are obtained from simulations in Griddler 2. Because we have not constructed a Griddler model for the multicrystalline cell, there are no corresponding simulation results to be added to Fig. 2(b). Nonetheless, some insights can be gleaned from the results.

For all light conditions in both cell types, the FF decreases with increase in $I_{\rm sc}$ due to greater power dissipation across series resistances. Probe bar shading causes notably smaller measured FFs. This decrease in FF arises since the shaded regions do not contribute to photogenerated current and the increase in irradiance power to maintain the target $I_{\rm sc}$ results in a distribution of the spatial photogeneration profile where the photogenerated current is generated further away from the current-collecting busbars. This increases effective series resistance $R_s$ and decimates the FF. Furthermore, the nonhomogeneous current distribution also causes internal current flow. The effect of nonuniform light fields is less straightforward and depends on the light profile relative to the busbars. In the above-mentioned case, they result in slightly higher FFs being measured which can partially mitigate the effect of probe bar shading. The impact of various nonuniform light fields and probe bar shading during *I–V* characterization can be examined in greater detail using Griddler 2.

### *B. Understanding the Impact of Nonuniform Irradiance Using Griddler*

Fig. 3(a) shows four nonuniform irradiance profiles chosen for further analysis in Griddler 2. Light field A consists of regions of variable intensity intermixed together; B consists of a radial profile with light intensity decreasing away from the center; C and D are linear light fields increasing from left-to-right and top-to-bottom, respectively.

For the nonuniform irradiance profiles in Fig. 3(a), the simulated $V_{\rm oc}$ maps are shown in Fig. 3(b). Regions under more intense illumination experience higher photogeneration rates and

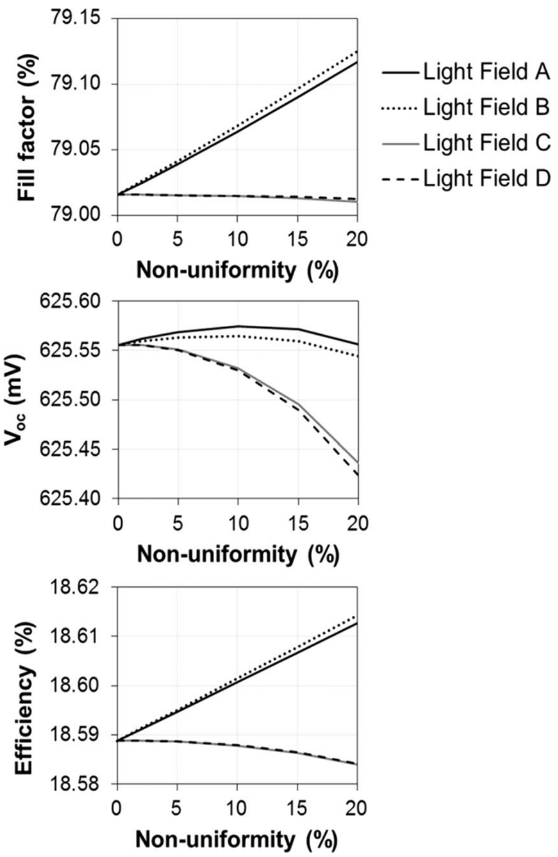


Fig. 4. Variation of fill factor (FF), open-circuit voltage ($V_{\rm oc}$), and efficiency with nonuniformity of the various light fields shown in Fig. 3(a).

possess higher concentrations of excess carriers, which lead to greater splitting of the quasi-Fermi levels than darker regions. Consequently, a spatial distribution of the open-circuit voltage $V_{\rm oc}$ arises with more brightly illuminated regions having a high $V_{\rm oc}$.

It is crucial to note that in addition to the irradiance nonuniformity, the specific irradiance profile has a strong influence on the measured *I–V* parameters. The dependence of FF, $V_{\rm oc}$, and efficiency on these two influences is shown in Fig. 4. Even with the same nonuniformity, the *I–V* parameters can vary to different extents. For instance, while there is only a small difference in the cell parameters between light fields A and B, and between C and D for the range of nonuniformity from 0 to 0.2, the parameters differ significantly between the two groups. Furthermore, while the FF of cells in A and B increases with nonuniformity with $V_{\rm oc}$ remaining more or less constant, the FF of C and D remains approximately constant as $V_{\rm oc}$ drops slightly. As a result, the measured efficiency of cells exposed to A and B is expected to increase with the nonuniformity, while that in C and D decreases slightly.

The increase in FF in light fields A and B, compared to C and D, is attributed to a higher concentration of brightly illuminated regions near the highly conductive busbars and less at the solar cell periphery. Even though the total $I_{\rm sc}$ is kept constant (by adjusting the total incident power), more current is photogenerated near the busbar in A and B. The currents travel a shorter lateral distance to the busbars for collection. This reduces the effective series resistance experienced by the current, thereby improving the FF. The effect is more pronounced with greater nonuniformity, since even more light and hence photogenerated current is situated close to the busbars and less at the periphery. $V_{\rm oc}$ changes little in A and B, since less current is photogenerated at the periphery, which is a region of higher recombination. The net effect is thus an overestimation of the cell efficiency with greater light nonuniformity.

In light fields C and D, the concentration of light near the edge of the solar cell contributes to a greater lateral distance travelled by the current to the bus bar and hence higher effective series resistance and lower FF. Also, higher peripheral recombination results due to the higher current density there. The net effect is thus an underestimation of the cell efficiency.

To better appreciate the effect of light nonuniformity during bare solar cell *I–V* measurement, the *I–V* characteristics of a typical three-bus bar monocrystalline Si wafer solar cell under 140 randomly generated inhomogeneous light fields with a range of nonuniformity from 0 to 20% are simulated in Griddler. Fig. 5(a) shows 16 of these simulated fields. The scatter plots for the FF, $V_{\rm oc}$, and efficiency are shown in Fig. 5(b), while the results are summarized in Table I.

It can be seen that with a large pool of simulated light fields, the standard deviation of FF, $V_{\rm oc}$, and efficiency increases in an increasing manner with increasing light field nonuniformity. For solar simulators with IEC 60904-9 class A classification for irradiance nonuniformity (2%), the standard deviation in FF is small at just 0.002% and is thus not a big issue. However, at 20% light field nonuniformity, the standard deviation in FF can be up to 0.19%. That is, for highly nonuniform light fields, simply specifying the nonuniformity is inadequate in describing the characteristics of a light field. This is because depending on how the irradiance is distributed over the light field, the measured *I–V* parameters, especially the FF, can differ significantly, thereby increasing the uncertainty of the measurement.

### *C. Impact on Large Busbar Shadings Affecting the Solar Cell Efficiency*

The recent trend of increasing the number of busbars (from the conventional three) on Si wafer solar cells to reduce series resistance losses requires a corresponding reduction in the busbar width to keep shading losses under control. This brings out the shading effect exerted by the probe-bars used for contacting the top surface of the bar solar cell during *I–V* measurement. Probe-bar shading cannot be easily avoided due to the finite thickness and height of the probe-bars, misalignment between probe bar and busbar, and divergence of the incident irradiance. While the irradiance can be adjusted to obtain probe-bar-contacted $I_{\rm sc}$ close to the 1-sun Kelvin probe values to compensate for probe-bar shading, the effects of the inadvertent shading deserves further examination.

The impact of probe bar shading at the busbars of a solar cell was again examined using Griddler but with a uniform incident light intensity. The definition of shading overfill at the cell busbar is illustrated in Fig. 6(a), while the simulated

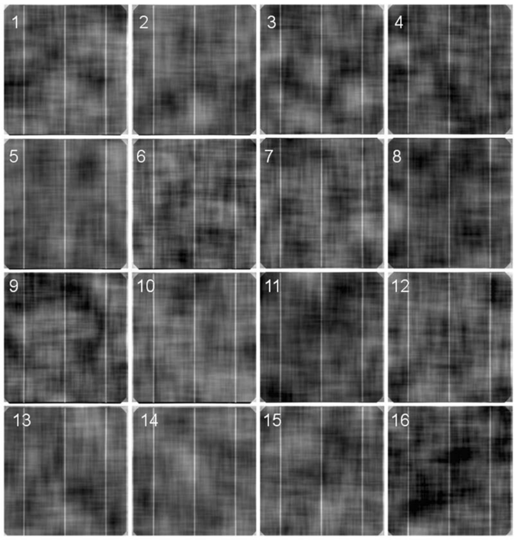


(a)

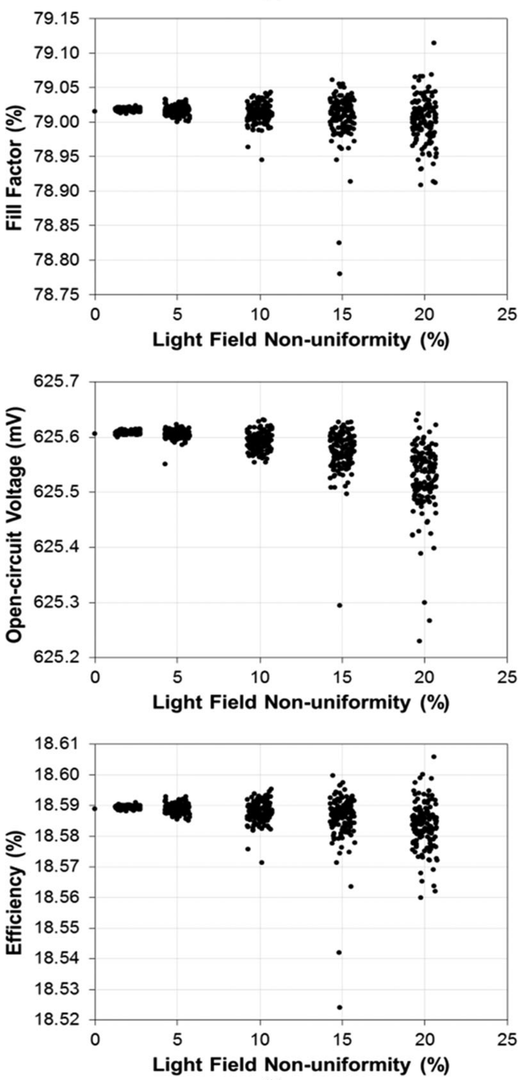


(b)

Fig. 5. (a) Sixteen of the random light fields simulated in Griddler. (b) Scatter plots of the fill factor, open-circuit voltage, and efficiency under various light fields at different light field nonuniformities.

TABLE I
*I–V* RESULTS UNDER VARIOUS LIGHT FIELDS SIMULATED IN GRIDDLER

| Light field nonuniformity (%) | Fill factor (%) Mean | Fill factor (%) Standard deviation | Open-circuit voltage (mV) Mean | Open-circuit voltage (mV) Standard deviation | Efficiency (%) Mean | Efficiency (%) Standard deviation |
|---|---|---|---|---|---|---|
| 0 | 79.016 | 0.000 | 625.556 | 0.000 | 18.589 | 0.000 |
| 2 | 79.018 | 0.002 | 625.558 | 0.003 | 18.589 | 0.000 |
| 5 | 79.017 | 0.006 | 625.556 | 0.009 | 18.589 | 0.001 |
| 10 | 79.014 | 0.015 | 625.542 | 0.015 | 18.588 | 0.004 |
| 15 | 79.007 | 0.037 | 625.524 | 0.040 | 18.586 | 0.009 |
| 20 | 78.975 | 0.186 | 625.473 | 0.065 | 18.577 | 0.045 |

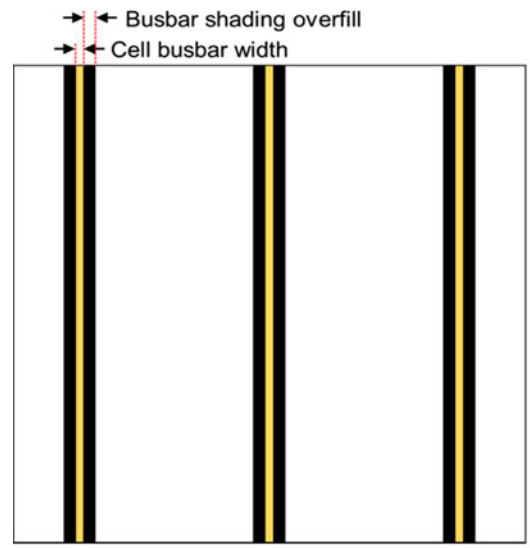


(a)

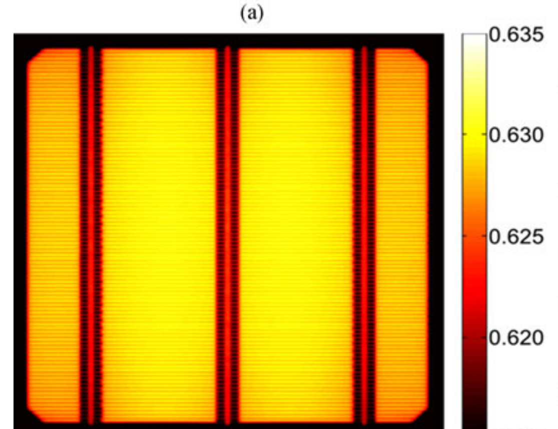


(b)

Fig. 6. (a) Schematic representation showing the busbar shading overfill. (b) A typical simulated open-circuit voltage map arising from shading at the busbars.

open-circuit voltage map is shown in Fig. 6(b). The regions adjacent to the busbars being shaded do not photogenerate carriers and thus result in zero open-circuit voltage. Due to higher recombination occurring at the cell periphery, $V_{\mathrm{oc}}$ in this region is reduced, thereby accounting for the darker contrast here. The areas between the three busbars and away from the edges thus possess the highest range of $V_{\mathrm{oc}}$.

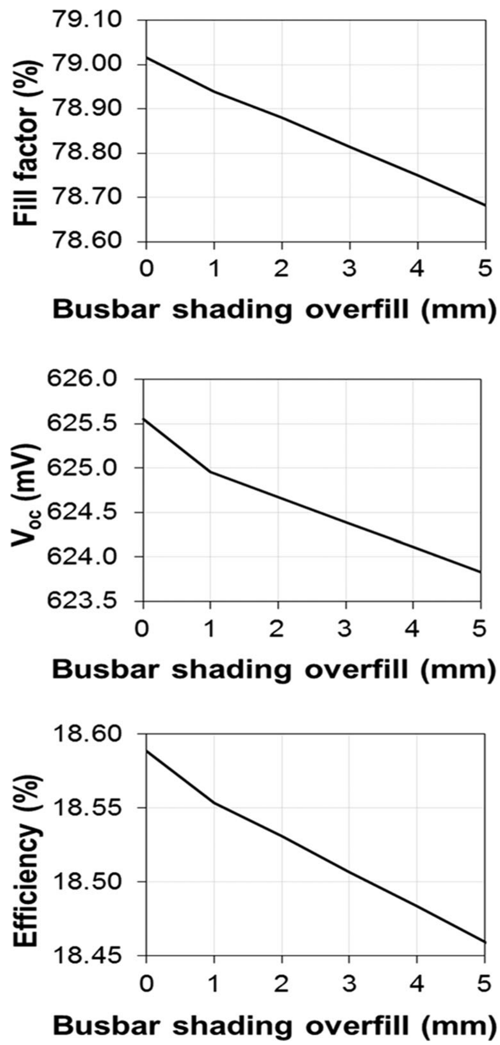


Fig. 7. Variation of fill factor (FF), open-circuit voltage ($V_{\rm oc}$), and efficiency with busbar shading overfill.

Fig. 7 charts the dependence of the FF, $V_{\rm oc}$, and efficiency on shading near the busbars. The FF drops with increasing busbar shading overfill because the photogenerated current becomes located increasingly further away from the busbar and thus have to travel greater lateral distances to reach the busbar for collection. This increases the effective series resistance as mentioned earlier and thus causes the FF drop. For shading overfill typical of conventional *I–V* measurement setups ($\sim$1.5 mm), the FF drop of $\sim$0.10% is not insignificant. Moreover, if busbar widths continue to shrink in multiple-busbar metallization patterns and probe bar widths remain approximately constant, it is expected that greater underestimation of FFs will result. Furthermore, the shaded regions do not photogenerate current and drag down the overall $V_{\rm oc}$. This is because internal currents flow within the nonuniformly illuminated cell even though the cell is in open-circuit. Voltage drop arises as the current flows through the internal resistance of the shaded region. [11] The ensuing voltage drop increases with greater busbar shading overfill. The overall effect is thus a decrease in the efficiency.

## V. Summary

Nonuniform illumination and probe bar shading were experimentally implemented during *I–V* measurement of Si wafer solar cells. The effects were examined in greater detail using Griddler 2, a finite element analysis software developed at the Solar Energy Research Institute of Singapore. The light *I–V* characteristics, particularly the FF, depend on the specific irradiance profiles relative to the current-collecting busbars due to effects on the effective series resistance $R_s$. The effect is slight for small light nonuniformities (IEC 60904 Class A nonuniformity classification or $<$2%) but for light nonuniformities up to 20%, the standard deviation in the FF can reach 0.19% absolute. Probe bar shading directly leads to an underestimation of the measured FF and open-circuit voltage due to higher effective series resistance and voltage drop in the shaded region, respectively. For typical busbar shading overfill of 1.5 mm, the drop in FF, $V_{\rm oc}$, and efficiency is not insignificant. With the trend of increasing busbar number and a corresponding shrinkage in busbar width, underestimation of the *I–V* parameters is expected to be more severe since reductions in probe bar width and dimension may be limited.

## References

[1] *Edition 2.0 Part 9: Solar Simulator Performance Requirements*, IEC 60904-9, 2008.

[2] W. Warta *et al.*, “Precise measurement of solar cell performance in production,” in *Proc. 24th Eur. Photovolt. Sol. Energy Conf. Exhib.*, Sep. 2009, pp. 21–25.

[3] J. Hohl-Ebinger, D. Grote, B. Hund, A. Mette, and W. Warta, “Contacting bare solar cells for STC measurements,” in *Proc. 23th Eur. Photovolt. Sol. Energy Conf. Exhib.*, Sep. 2008, pp. 1–5.

[4] H. Baig, K. C. Heasman, and T. K. Mallick, “Non-uniform illumination in concentrating solar cells,” *Renew. Sustain. Energy Rev.*, vol. 16, no. 8, pp. 5890–5909, 2012.

[5] H. Pfeiffer and M. Bihler, “The effects of non-uniform illumination of solar cells with concentrated light,” *Sol. Cells*, vol. 5, no. 3, pp. 293–299, Mar. 1982.

[6] J. Wong, “Griddler: Intelligent computer aided design of complex solar cell metallization patterns,” in *Proc. 39th IEEE Photovolt. Spec. Conf.*, 2013, pp. 933–938.

[7] J. Wong, R. Sridharan, and V. Shanmugam, “Quantifying edge and peripheral recombination losses in industrial silicon solar cells,” *IEEE Trans. Electron Devices*, vol. 62, no. 11, pp. 3750–3755, Nov. 2015.

[8] *Edition 3.0 Part 7: Computation of the Spectral Mismatch Correction for Measurements of Photovoltaic Devices*, IEC 60904-7, 2008.

[9] *Edition 2.0 Part 3: Measurement Principles for Terrestrial Photovoltaic (PV) Solar Devices With Reference Spectral Irradiance Data*, IEC 60904-3, 2008.

[10] J. Wong and R. Sridharan, “Griddler 2: Two dimensional solar cell simulator with facile definition of spatial distribution in cell parameters and bifacial calculation mode,” in *Proc. 42th IEEE Photovolt. Spec. Conf.*, 2015.

[11] A. Cuevas and S. López-Romero, “The combined effect of non-uniform illumination and series resistance on the open-circuit voltage of solar cells,” *Sol. Cells*, vol. 11, no. 2, pp. 163–173, Mar. 1984.

Authors’ photographs and biographies not available at the time of publication.